

RSC Advances

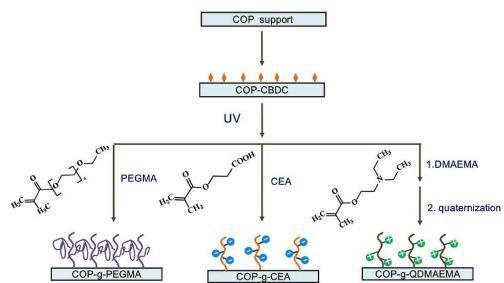


This is an *Accepted Manuscript*, which has been through the Royal Society of Chemistry peer review process and has been accepted for publication.

Accepted Manuscripts are published online shortly after acceptance, before technical editing, formatting and proof reading. Using this free service, authors can make their results available to the community, in citable form, before we publish the edited article. This *Accepted Manuscript* will be replaced by the edited, formatted and paginated article as soon as this is available.

You can find more information about *Accepted Manuscripts* in the [Information for Authors](#).

Please note that technical editing may introduce minor changes to the text and/or graphics, which may alter content. The journal's standard [Terms & Conditions](#) and the [Ethical guidelines](#) still apply. In no event shall the Royal Society of Chemistry be held responsible for any errors or omissions in this *Accepted Manuscript* or any consequences arising from the use of any information it contains.



TOC

Cycloolefin polymer was modified via surface-initiated photoiniferter-mediated polymerization for suppressing bioadhesion.

Cite this: DOI: 10.1039/c0xx00000x

www.rsc.org/xxxxxx

ARTICLE TYPE

Surface modification of cycloolefin polymer via surface-initiated photoiniferter-mediated polymerization for suppressing bioadhesion

Jiao Ma,^{a,b} Shifang Luan,^{*a} Jing Jin,^a Lingjie Song,^{a,b} Shuaishuai Yuan,^{a,b} Wanling Zheng^a and Jinghua Yin^{*a}

Inert cycloolefin polymers (COPs), which possess excellent optical properties, are a series of ideal material for fabricating cheap disposable biosensor platforms. However, their antibioadhesion properties are expected to be improved prior to their applications as a biosensor support. In this study, for the first time the COP supports were modified with well-controlled neutral, anionic and cationic polymer brushes via surface-initiated photoiniferter-mediated polymerization. This graft polymerization was confirmed by infrared spectroscopy, and X-ray photoelectron spectroscopy. The antibioadhesion properties of the modified supports were evaluated through a series of biological experiments. It was found that among these modified samples, the anionic poly(2-carboxyethyl acrylate)-modified COP supports presented the best antibioadhesion performances, i.e., suppressing protein adsorption, platelet adhesion and red blood cell attachment.

Introduction

Polymers including polycarbonate,¹ poly(ethylene terephthalate),² polystyrene,³ and cycloolefin polymer (COP)⁴⁻⁶ are now regarded as attractive bioassay substrates owing to their ease of fabrication, and low cost. Among these developed polymers, COP presents excellent optical properties, e.g., high transparency, low birefringence, low autofluorescence, and absence of UV absorption, which render it particularly well-suited for the disposable sophisticated microchip platforms.⁷⁻¹¹

It is well acknowledged that plasma proteins will be adsorbed on hydrophobic surfaces at the initial stage, followed by platelet adhesion, the activation of the coagulation pathways, and final thrombus formation.¹² Thus, the substrate materials of bioassays are required to possess good antibioadhesion properties, otherwise it may result in a low targeting efficiency of diagnostics in crude blood.^{13, 14} As such, the antibioadhesion performances of the hydrophobic COP are expected to be improved via surface modification prior to its application as a biosensor support.¹⁵

Surface modification is a promising methodology for the functionalization of polymeric substrates without affecting their bulk properties.¹⁶⁻¹⁹ Notably, surface-initiated photopolymerization has significant advantages, such as fast reaction rate, simple equipment, and ease of industrialization.^{20, 21} A novel surface-initiated photoiniferter-mediated polymerization (SI-PIMP) has been developed recently, and its controlled polymerization nature is particularly attractive.²²⁻²⁴ Compared with surface-initiated atom transfer radical polymerization (SI-ATRP), a key advantage of SI-PIMP is that it just relies on UV irradiation to conduct graft reactions, thereby avoiding the requirement for removing toxic catalyst complexes.²⁵ Benetti et al. reported that the poly(*N*-isopropylacrylamide) (PNIPAM) brushes with the uniform chain length could be grafted on a gold substrate using a newly developed disulfide-containing

photoiniferter.²² Based on the SI-PIMP method, a series of two-layer zwitterionic architectures, consisting of a bottom layer for ultra low fouling and an upper layer for high protein loading, were constructed by Jiang group. It was found that the antibody binding capacity and antigen detection of the as-prepared samples were superior to that prepared by the SI-ATRP approach.^{26, 27}

A desired antibioadhesion surface can be fabricated by introducing various hydrophilic substances, such as zwitterionic materials,²⁸⁻³² heparin,³³⁻³⁵ poly(ethylene glycol) (PEG),³⁶⁻⁴⁰ and poly(vinylpyrrolidone) (PNVP).⁴¹⁻⁴⁵ Up to now, the surface modification with the charged polymer brushes have not been thoroughly understood yet because of the limited research.⁴⁶⁻⁴⁸

In this work, for the first time a COP support was modified with neutral, anionic, and cationic polymer brushes via the controlled SI-PIMP strategy. The antibioadhesion properties of the modified supports were evaluated by a series of biological experiments, including protein adsorption, platelet adhesion, and red blood cell attachment.

Experimental section

Materials and reagents

Cycloolefin polymer (COP) Zeonex 690R granules were provided by ZEON Corp.. 4-(Chloromethyl) benzoyl chloride (CMBC, >98.0%) was purchased from TCI Shanghai. Poly(ethylene glycol) methacrylate (PEGMA) monomer ($M_n = 360$), 2-carboxyethyl acrylate (CEA), 2-(dimethylamino) ethyl methacrylate (DMAEMA), and sodium diethyldithiocarbamate trihydrate (DETC, >99.0%) were purchased from Sigma-Aldrich. Phosphate buffer solution (PBS, pH = 7.4), bovine serum albumin (BSA), bovine serum fibrinogen (BFg), and sodium dodecyl sulfate (SDS) were purchased from Dingguo Biotechnology. Alexa 488-labeled human fibrinogen (A488-HFg) was purchased from Life Technology. PEGMA, DMAEMA, and CEA were passed through an alumina column to remove the inhibitor before

use. Other reagents were all AR grade and used as received without further purification.

Photoiniferter immobilization

The COP supports were subjected to oxygen plasma (DT-03 plasma apparatus, Suzhou Omega Technology) under the condition of 90 W and 16 Pa for 60 s. The plasma-treated supports were then immersed in an anhydrous ethyl acetate solution of CMBC [10% (v/v)] and pyridine [3% (v/v)] for 24 h under an anhydrous atmosphere to obtain CMBC-immobilized samples (denoted as COP-CMBC). They were then immersed into an ethanolic solution of DETC [10% (m/v)] for 48 h at 37 °C. After thoroughly rinsing with ethanol and deionized water, the as-prepared supports were denoted as COP-CBDC.

Preparation of neutral, anionic, and cationic polymer brushes modified-COP supports

To conduct SI-PIMP on the COP-CBDC supports, the aqueous solution of monomers (10 vol%), i.e., PEGMA, CEA, or DMAEMA, were degassed with nitrogen stream for 30 min. The COP-CBDC supports were placed on a quartz plate, coated with the degassed solution, and finally covered with another quartz plate. The sandwich systems were exposed to UV light (high-pressure mercury lamp, 400 W, main wavelength 380nm) for a desired time. The obtained supports were denoted as COP-g-PEGMA, COP-g-CEA, and COP-g-DMAEMA, respectively.

For obtaining the cationic polymer brushes modified-supports, the COP-g-DMAEMA supports were soaked in an ethyl acetate solution of ethyl bromide [20% (v/v)] at 30 °C for 3 h to conduct the quarternization reaction. The as-prepared sample was denoted as COP-g-QDMAEMA.

Surface chemistry characterization

ATR-FTIR curves were examined by Bruker Vertex 70 Fourier transform infrared spectroscopy installed with an attenuated total reflection (ATR) unit (crystal 45°) at a resolution of 4 cm⁻¹ for 32 scans. The surface elemental composition of the samples was determined by X-ray photoelectron spectroscopy (XPS, VG Scientific ESCA MK II Thermo Avantage V 3.20 analyzer) with an Al K α ($h\nu = 1486.6$ eV) anode mono-X-ray source at a detection angle of 90°. The spectra were collected over a wide range of 0-1200 eV, and the high-resolution C 1s, N 1s and Br 3d spectras were provided. The atomic concentrations of the elements were calculated according to the peak-area ratios.

Wettability and surface energy

For the static water contact angle (WCA) measurement, the samples were dried under vacuum overnight and then examined with a contact angle goniometer (KRÜSS GmbH) at room temperature by the sessile drop method. At least three measurements were conducted for calculating the average WCA value of each sample. The surface energy was calculated according to the reported equation in the literature.⁴¹

Nonspecific protein adsorption test

The samples with a surface area of 0.9 cm² were placed in a 24-well tissue culture plate, and equilibrated with a PBS solution overnight, followed by incubating in a PBS solution containing BSA or BFG (1.0 mg/mL) at 37 °C for 2 h. Each sample was sequentially rinsed five times with fresh PBS, immersed into an aqueous solution of SDS (1.0 wt%), and sonicated at 37 °C for 20 min to remove the adsorbed proteins from the substrate completely. The concentration of the protein in the SDS solution were determined with a micro BCATM protein assay reagent kit based on the bicinchoninic acid (BCA) method. The optical density was measured using a micro plate reader (TECAN GENIOS, Austria) at 562 nm.

As for the fluorescent A488-HFg adsorption evaluation, the samples were incubated in a PBS solution containing A488-HFg (100 μ g/mL) at 4 °C for 12 h. After rinsing with PBS, drying with a nitrogen flow, the samples were finally examined with a confocal laser scanning microscopy (Zeiss, LSM 700) under the same condition (Intensity: 3.0; Pinhole: 320.9; Gain: 788).

The evaluation of platelet and red blood cell (RBC) adhesion

The samples were placed in a 24-well tissue culture plate, and equilibrated with a PBS solution for 2 h at 37 °C. Then 20 μ L of fresh platelet-rich plasma or RBC suspension solution from a healthy rabbit was dripped onto the center of the samples, and incubated at 37 °C for 2 h. After rinsing three times with a PBS solution, the platelets or RBCs adhered on the surfaces were fixed with a PBS solution of glutaraldehyde (2.5 wt%) at 4 °C for 4 h. Finally, the samples were rinsed several times with a PBS solution and freeze-dried under a vacuum, followed by observing with a field emission scanning electron microscopy (FESEM, XL 30 ESEM FEG, FEI Company).

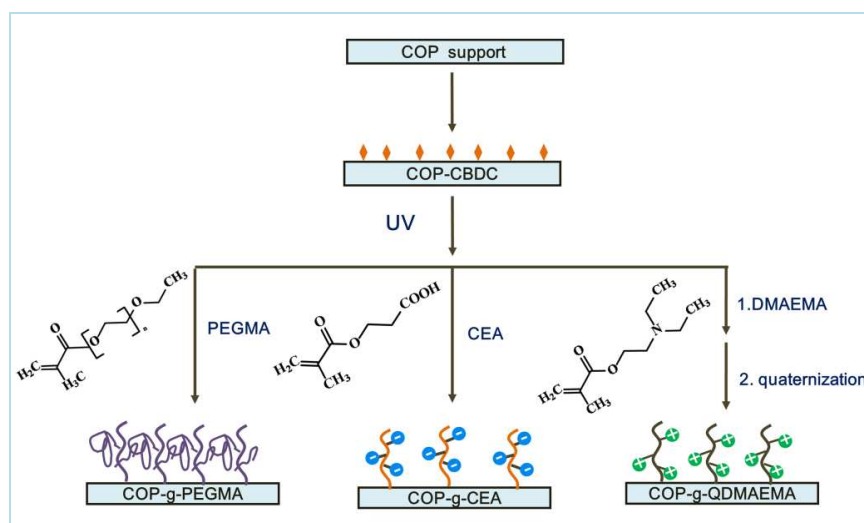
Results and discussion

Although COP is regarded as an ideal material to fabricate a biosensor for point-of-care applications because of its excellent optical properties, its antibioadhesion properties are expected to be improved via surface modification. As illustrated in Scheme 1, an intergrated SI-PIMP surface modification process was developed to modify the hydrophobic and chemical-inert COP supports with a well-controlled graft layer. The samples were first activated by O₂ plasma to form the active species including hydroxyl, carboxyl and peroxide groups, followed by initiator attachment through reacting with CMBC and DETC in succession. The following SI-PIMP of PEGMA, CEA, and DMAEMA was conducted under UV irradiation. In contrast to SI-ATRP, SI-PIMP not only inherits the merits of the conventional photopolymerization, e.g., simple equipment, and fast reaction rate, but also has a controlled polymerization nature, and tolerates a wide range of monomers.

Cite this: DOI: 10.1039/c0xx00000x

www.rsc.org/xxxxxx

ARTICLE TYPE



Scheme 1. Preparation procedure of the neutral, cationic and anionic polymer brushes -modified COP supports.

Surface chemistry characterization

The chemical composition of the initiator-immobilized COP supports was characterized by XPS. Figure 1 shows the Cl 2p, S 2p, and N 1s core-level spectra of the COP, COP-CMBC, and COP-CBDC surfaces. A Cl 2p signal at about 198 eV, attributed to the benzyl chloride, appeared in the COP-CMBC surface. After reacting with DETC, the intensity of the Cl peak weakened, and the corresponding Cl/C ratio decreased from 1.52% to 0.94% (Table 1). Meanwhile, the S/C ratio increased from 0.63% to 1.10%, and the N/C ratio increased from 2.48% to 3.27% because of the introduction of the -S-C-S=N structure.

The SI-PIMP of PEGMA, CEA and DMAEMA was performed on the COP-CBDC supports to prepare the neutral, anionic, and cationic polymer brushes-modified samples. The ATR-FTIR spectra of the samples were shown in Figure 2. As for the COP-g-PEGMA sample, the characteristic adsorption bands of the C=O groups at about 1723 cm⁻¹ confirmed the surface graft polymerization of PEGMA. In the case of the COP-g-CEA samples, two characteristic peaks corresponding to C=O and COO⁻ groups appeared at 1734 cm⁻¹ and 1585 cm⁻¹, respectively. As for the COP-g-DMAEMA sample, there is also a

characteristic absorption band at about 1729 cm⁻¹ due to the C=O stretching vibration.

The cationic quaternary ammonium monomer can not be grafted from the COP supports probably because the quaternary ammonium structures render the inactivation of the photoiniferter. Thus, the DMAEMA-modified supports were first prepared, followed by the quaternization of DMAEMA polymer brushes to obtain the cationic polymer brushes-modified samples in this work. Figure 3 presents the C 1s, N 1s, and Br 3d XPS core-level spectra of the samples before and after quaternization. The high-resolution Cls curve was decomposed into four peaks: a C-C peak at about 284.5 eV, a C-N peak at about 285.7 eV, a C-O

Table 1. The elemental compositions of the COP supports

| sample | Cl/C (%) | S/C (%) | N/C (%) |
|----------|----------|---------|---------|
| COP | 0.07 | 0.09 | 0.87 |
| COP-CMBC | 1.52 | 0.63 | 2.48 |
| COP-CBDC | 0.94 | 1.10 | 3.27 |

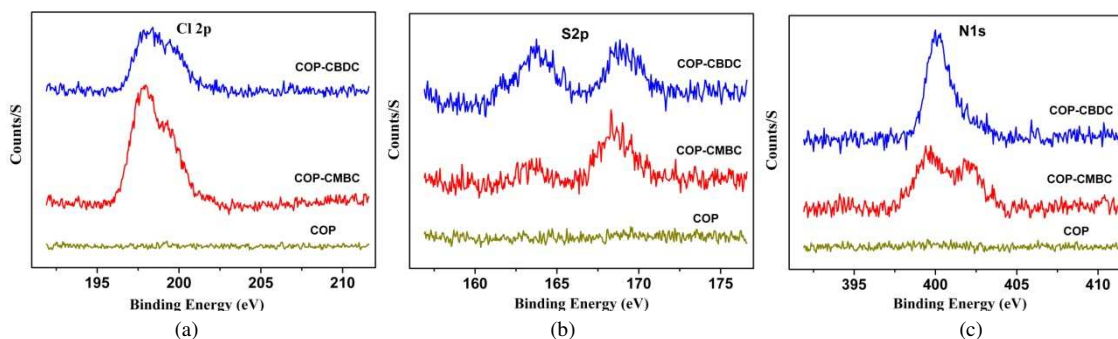


Figure 1. High-resolution XPS spectra of the samples before and after the immobilization of initiator: (a) Cl 2p spectra; (b) S 2p spectra; (c) N 1s spectra

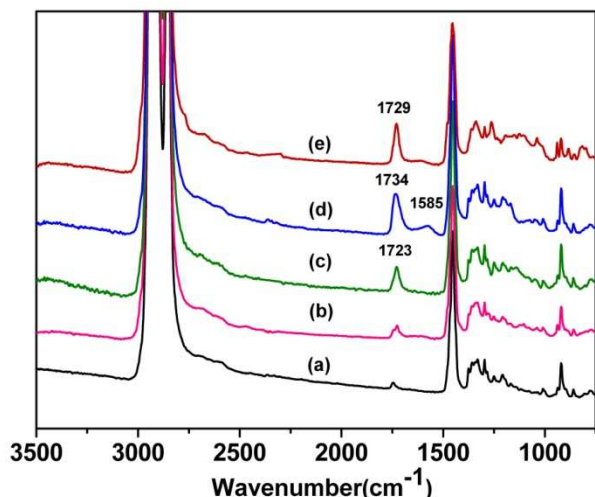


Figure 2. ATR-FTIR spectra of the COP supports: (a) virgin COP; (b) COP-CBDC; (c) COP-g-PEGMA; (d) COP-g-CEA; (e) COP-g-DMAEMA.

peak at about 286.6 eV, and a O=C-O peak at about 288.6 eV, respectively. Little change was observed for the C 1s spectra after the quarternization. The N 1s spectra had an obvious change with the appearance of an characteristic peak at about 402.2 eV attributed to C-N⁺ species, and a strong Br 3d signal at about 67.6 eV appeared in the COP-g-QDMAEMA samples, which confirmed the quarternization procedure.

Wettability and surface energy

Surface hydrophilicity is a significant property relating to the antibioadhesion of polymeric materials. Considering the effect of environment on the wettability, the modified supports were first dried under vacuum and then evaluated by the sessile WCA measurement.^{49,50} As shown in Figure 4, the virgin COP supports had a WCA of $96 \pm 2^\circ$, and a surface energy of $25 \pm 1 \text{ mJ/m}^2$. As for the COP-CBDC samples, the WCA decreased to $61 \pm 3^\circ$, and the surface energy increased to $47 \pm 1 \text{ mJ/m}^2$. After the graft polymerization of the hydrophilic PEGMA and CEA onto the COP surfaces, the WCAs decreased to $54 \pm 3^\circ$ and $26 \pm 6^\circ$, while the surface energies respectively increased to $51 \pm 1 \text{ mJ/m}^2$ and $66 \pm 2 \text{ mJ/m}^2$. Unexpectedly, the WCA of the COP-g-QDMAEMA samples increased to $82 \pm 3^\circ$, and the surface energy decreased to $34 \pm 2 \text{ mJ/m}^2$. The phenomena were probably attributed to the hydrophobicity from the N-alkylation.⁵¹

Nonspecific protein adsorption

The wettability of polymeric surfaces has a great impact on the protein adsorption behavior, which will cause the subsequent platelet adhesion, the activation of the coagulation pathways, and the final thrombus formation when contacting with blood. Protein adsorption as the initial process plays a key role in the above interlock procedures. Among the various plasma proteins, BSA is a small and highly abundant plasma protein with the slight ellipsoid shape ($14 \text{ nm} \times 4 \text{ nm} \times 4 \text{ nm}$), which is generally

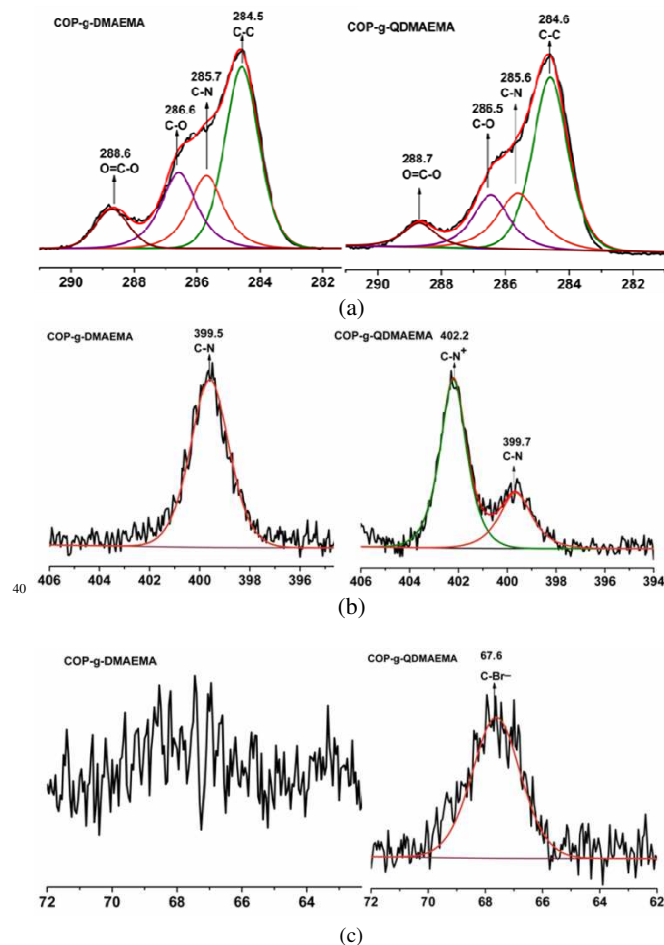


Figure 3. High-resolution XPS of the COP-g-DMAEMA and COP-g-QDMAEMA supports. (a) C 1s spectra; (b) N 1s spectra; (c) Br 3d spectra.

considered to be nonadhesive to platelet; in contrast, BFG is an adhesive protein with the rodlike structure ($47 \text{ nm} \times 5 \text{ nm} \times 5 \text{ nm}$), which will render coagulation, platelet activation and aggregation.⁵² Herein, BSA and BFG, are used as models for assessing the protein adsorption behavior on the modified COP supports. As shown in Figure 5, the amount of the protein adsorption on the COP-CBDC supports changed slightly despite of the increased hydrophilicity, compared with the virgin COP supports. As for the PEGMA-modified COP supports, they presented a great decrease of protein adsorption, probably because the hydration, and the chain mobility of the PEG polymer brushes prevent the proteins from approaching the substrates. Nearly no improvement on the resistance to protein adsorption was observed for the COP-g-QDMAEMA supports probably because of the electrostatic interaction between the negatively charged proteins and the positively charged surfaces. Notably, among these modified COP supports, the COP-g-CEA supports exhibited the most excellent antibioadhesion property with a decrease of BSA and BFG by 70% and 90%, respectively.

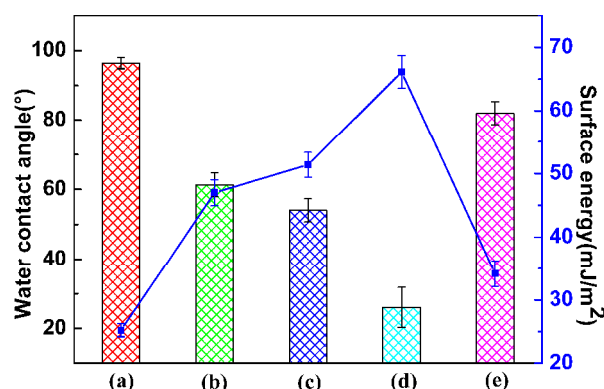


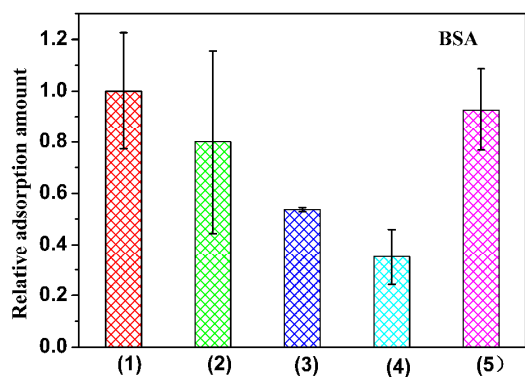
Figure 4. Water contact angle and surface energy of the COP supports: (a) virgin COP; (b) COP-CBDC; (c) COP-g-PEGMA; (d) COP-g-CEA; (e) COP-g-QDMAEMA. (error bars: standard deviations, $n = 3$).

It was attributed to the powerful ability of CEA to entrap water. The difference between the BSA and BFG adsorption behaviors on these surfaces may result from the different isoelectric point values and protein sizes.

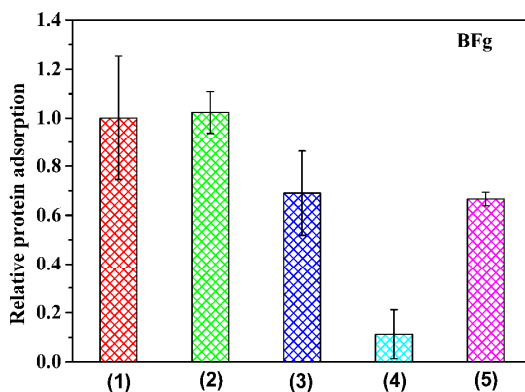
Furthermore, we investigated the A488-HFg adsorption behavior through fluorescence intensity scanning, which can directly provide the fluorescent images of the adsorbed proteins.^{31, 53} As shown in Figure 5 (c), the strong fluorescent image suggested that a large amount of A488-HFg adsorbed on

t h e

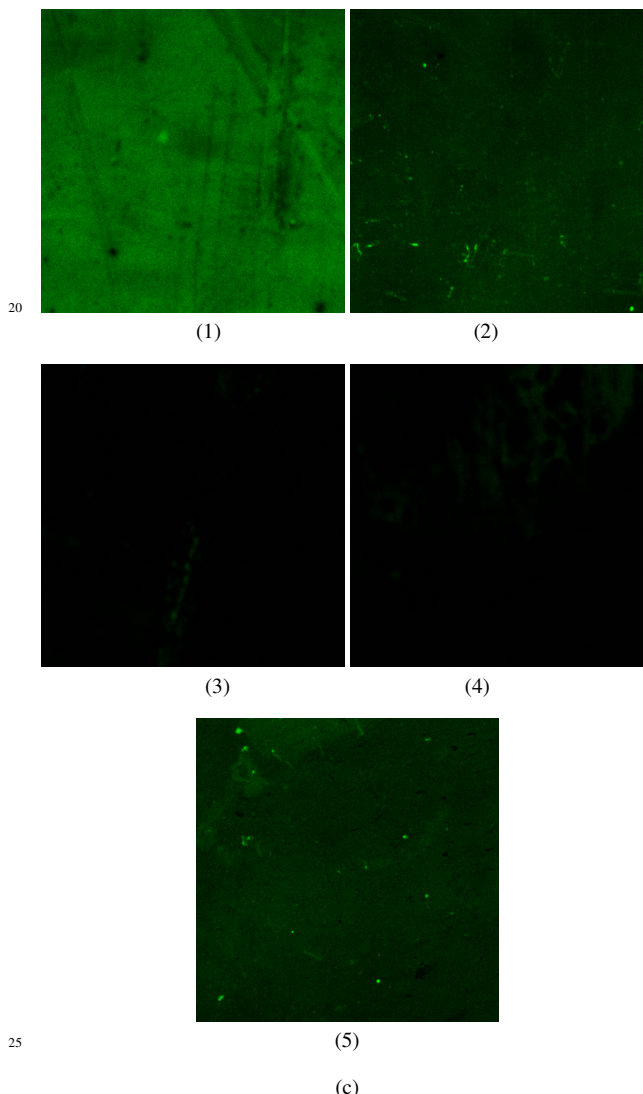
15



(a)



(b)



25

Figure 5. Adsorption of BSA (a), BFG (b) and A488-HFg (c) on the supports: (1) virgin COP; (2) COP-CBDC; (3) COP-g-PEGMA; (4) COP-g-CEA; (5) COP-g-QDMAEMA. (error bars: standard deviations, $n = 3$;
30 Picture area: $639.5 \mu\text{m} \times 639.5 \mu\text{m}$).

virgin COP supports, in contrast to the dark images of the PEGMA and CEA-modified supports. The medium fluorescence observed on the COP-CBDC and COP-g-QDMAEMA supports means that a large amount of HFg still adsorbed on the surfaces.

35 Platelet adhesion and RBC attachment

The platelet adhesion on polymeric materials mainly depends on the surface characteristics, e.g., surface free energy, wettability, charge density, and chemistry property. As shown in Figure 6, when contacting with platelet-rich plasma, a large number of platelets were adhered on the virgin COP and COP-CBDC supports. Most of these platelets are highly activated, as evidenced by the presence of pseudopodia. As for the PEGMA and CEA-modified supports, the hydrophilic chains of PEGMA and CEA were quickly hydrated, and therefore, just a few inactivated platelets were observed. Because of the attractive interaction and surface hydrophobicity (a WCA of 82°), a large number of activated platelets with long pseudopodia were

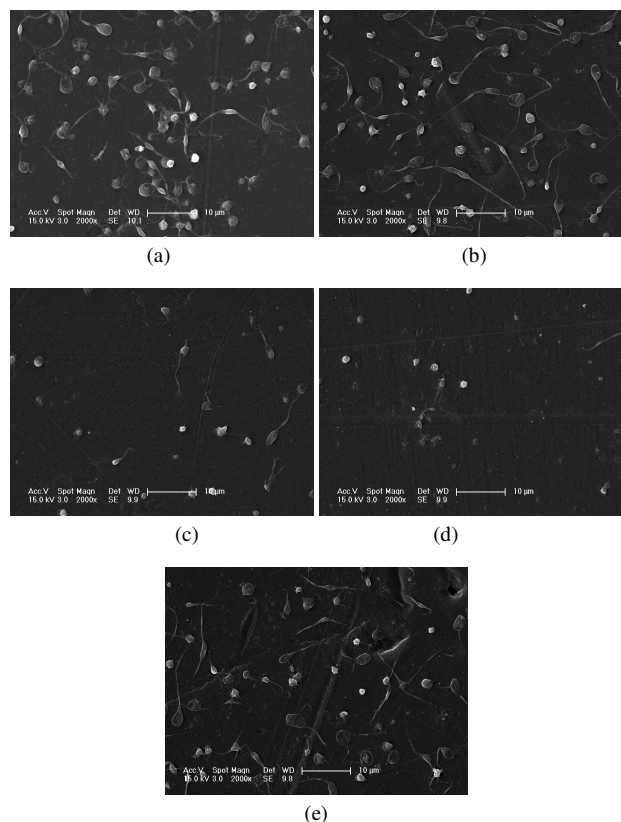


Figure 6. Platelet adhesion on the supports: (a) virgin COP; (b) COP-CBDC; (c) COP-g-PEGMA; (d) COP-g-CEA; (f) COP-g-QDMAEMA.

observed on the COP-g-QDMAEMA supports.

The attachment of RBCs on the surfaces from the whole blood is considered to be a challenging process, comparable to the platelet adhesion because these behaviors on the biosensor surfaces would occupy the antigen binding sites, resulting in a low targeting efficiency.⁵⁴ As presented in Figure 7, a lot of RBCs attached on the COP and COP-CBDC surfaces, in contrast to only a few cells on the hydrophilic COP-g-PEGMA and COP-g-CEA supports. Remarkably, a huge amount of RBCs were observed on the COP-g-QDMAEMA surfaces, which is consistent with the reported results that the cationic surfaces facilitate cell adhesion.⁵⁵

Conclusions

In this work, for the first time the COP supports were successfully functionalized with the neutral PEGMA, cationic QDMAEMA, and anionic CEA polymer brushes by the SI-PIMP approach. It was demonstrated that among the modified samples, the anionic COP-g-CEA supports presented the best antibioadhesion properties. Compared with the virgin COP supports, model protein adsorption of the COP-g-CEA supports were decreased by up to 90%. And the platelet adhesion, and red blood cell attachment were substantially suppressed on the COP-g-CEA supports. This study suggests that the excellent antibioadhesion properties of the CEA-modified COP supports will exhibit a great potential application in the immunoassay.

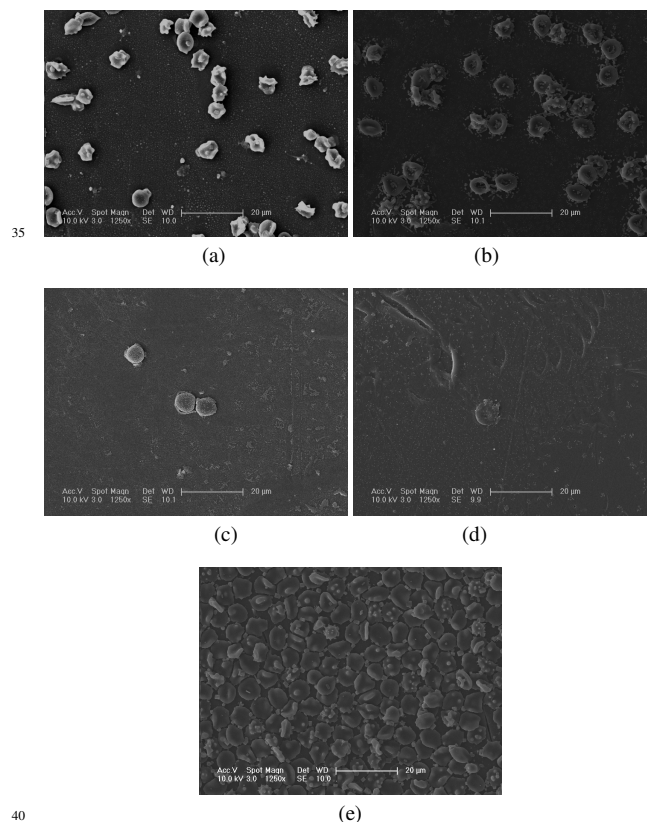


Figure 7. Red blood cells attachment on the supports: (a) virgin COP; (b) COP-CBDC; (c) COP-g-PEGMA; (d) COP-g-CEA; (f) COP-g-QDMAEMA.

Notes and references

- ^a State Key Laboratory of Polymer and Chemistry, Changchun Institute of Applied Chemistry, Chinese Academy of Sciences, Changchun 130022, People's Republic of China. Fax: +86 431 85262109; Tel: +86 431 85262109; E-mail: sfluan@ciac.ac.cn; yinhj@ciac.ac.cn
- ^b University of Chinese Academy of Sciences, Beijing 100049, People's Republic of China
- D. Yang, X. Niu, Y. Liu, Y. Wang, X. Gu, L. Song, R. Zhao, L. Ma, Y. Shao and X. Jiang, *Adv. Mater.*, 2008, **20**, 4770-4775.
- I. T. Hwang, I. S. Kuk, C. H. Jung, J. H. Choi, Y. C. Nho and Y. M. Lee, *ACS Appl. Mater. Interfaces*, 2011, **3**, 2235-2239.
- N. J. Alves, N. Mustafaoglu and B. Bilgicer, *Biosens. Bioelectron.*, 2013, **49**, 387-393.
- V. Gubala, R. P. Gandhiraman, C. Volcke, C. Doyle, C. Coyle, B. James, S. Daniels and D. E. Williams, *Analyst*, 2010, **135**, 1375-1381.
- S. Laib and B. D. MacCraith, *Anal. Chem.*, 2007, **79**, 6264-6270.
- R. P. Gandhiraman, C. Volcke, V. Gubala, C. Doyle, L. Basabe-Desmonts, C. Dotzler, M. F. Toney, M. Iacono, R. I. Nooney, S. Daniels, B. James and D. E. Williams, *J. Mater. Chem.*, 2010, **20**, 4116-4127.
- C. Jonsson, M. Aronsson, G. Rundstrom, C. Pettersson, I. Mendel-Hartvig, J. Bakker, E. Martinsson, B. Liedberg, B. MacCraith, O. Ohman and J. Melin, *Lab Chip*, 2008, **8**, 1191-1197.
- G. A. Diaz-Quijada, R. Peytavi, A. Nantel, E. Roy, M. G. Bergeron, M. M. Dumoulin and T. Veres, *Lab Chip*, 2007, **7**, 856-862.
- M. Geissler, E. Roy, G. A. Diaz-Quijada, J. C. Galas and T. Veres, *ACS Appl. Mater. Interfaces*, 2009, **1**, 1387-1395.
- E. Roy, M. Geissler, J. C. Galas and T. Veres, *Microfluid. Nanofluid.*, 2011, **11**, 235-244.
- E. Roy, J. C. Galas and T. Veres, *Lab Chip*, 2011, **11**, 3193-3196.

- 12 H. Yang, S. Luan, J. Zhao, H. Shi, X. Li, L. Song, J. Jin, Q. Shi, J. Yin, D. Shi and P. Stagnaro, *Polymer*, 2012, **53**, 1675-1683.
- 13 H. Vaisocherová, W. Yang, Z. Zhang, Z. Cao, G. Cheng, M. Piliarik, J. i. Homola and S. Jiang, *Anal. Chem.*, 2008, **80**, 7894-7901.
- 14 N. D. Brault, C. Gao, H. Xue, M. Piliarik, J. Homola, S. Jiang and Q. Yu, *Biosens. Bioelectron.*, 2010, **25**, 2276-2282.
- 15 S. Roy, C. Y. Yue, S. S. Venkatraman and L. L. Ma, *J. Mater. Chem.*, 2011, **21**, 15031-15040.
- 16 Q. A. Yu, Y. X. Zhang, H. W. Wang, J. Brash and H. Chen, *Acta Biomater.*, 2011, **7**, 1550-1557.
- 17 F. He, B. Luo, S. Yuan, B. Liang, C. Choong and S. O. Pehkonen, *RSC Adv.*, 2014, **4**, 105-117.
- 18 A. Schulze, M. F. Maitz, R. Zimmermann, B. Marquardt, M. Fischer, C. Werner, M. Went and I. Thomas, *RSC Adv.*, 2013, **3**, 22518-22526.
- 19 M. Kumar and M. Ulbricht, *RSC Adv.*, 2013, **3**, 12190-12203.
- 20 U. Edlund, M. Källrot and A. C. Albertsson, *J. Am. Chem. Soc.*, 2005, **127**, 8865-8871.
- 21 M. Källrot, U. Edlund and A. C. Albertsson, *Biomaterials*, 2006, **27**, 1788-1796.
- 22 E. M. Benetti, S. Zapotoczny and G. J. Vancso, *Adv. Mater.*, 2007, **19**, 268-271.
- 23 E. M. Benetti, E. Reimhult, J. de Bruin, S. Zapotoczny, M. Textor and G. J. Vancso, *Macromolecules*, 2009, **42**, 1640-1647.
- 24 A. Li, S. N. Ramakrishna, T. Schwarz, E. M. Benetti and N. D. Spencer, *ACS Appl. Mater. Interfaces*, 2013, **5**, 4913-4920.
- 25 J. E. Krause, N. D. Brault, Y. Li, H. Xue, Y. Zhou and S. Jiang, *Macromolecules*, 2011, **44**, 9213-9220.
- 26 C. J. Huang, N. D. Brault, Y. Li, Q. Yu and S. Jiang, *Adv. Mater.*, 2012, **24**, 1834-1837.
- 27 C. J. Huang, Y. T. Li and S. Y. Jiang, *Anal. Chem.*, 2012, **84**, 3440-3445.
- 28 B. Byambaa, T. Konno and K. Ishihara, *Colloids Surface., B*, 2012, **99**, 1-6.
- 29 M. Wang, J. Yuan, X. B. Huang, X. M. Cai, L. Li and J. Shen, *Colloids Surface., B*, 2013, **103**, 52-58.
- 30 W. W. Yue, H. J. Li, T. Xiang, H. Qin, S. D. Sun and C. S. Zhao, *J. Membr. Sci.*, 2013, **446**, 79-91.
- 31 N. D. Winblade, I. D. Nikolic, A. S. Hoffman and J. A. Hubbell, *Biomacromolecules*, 2000, **1**, 523-533.
- 32 J. J. Huang, D. Wang, Y. Lu, M. F. Li and W. L. Xu, *RSC Adv.*, 2013, **3**, 20922-20929.
- 33 U. Edlund, S. Danmark and A. C. Albertsson, *Biomacromolecules*, 2008, **9**, 901-905.
- 34 K. Zhang, J. A. Li, K. Deng, T. Liu, J. Y. Chen and N. Huang, *Colloids Surf., B*, 2013, **108**, 295-304.
- 35 S. Nie, M. Tang, C. Cheng, Z. Yin, L. Wang, S. Sun and C. Zhao, *Biomater. Sci.*, 2014, **2**, 98-109.
- 36 D. Li, H. Chen, W. G. McClung and J. L. Brash, *Acta Biomater.*, 2009, **5**, 1864-1871.
- 37 F. J. Xu, K. G. Neoh and E. T. Kang, *Prog. Polym. Sci.*, 2009, **34**, 719-761.
- 38 D. Li, H. Chen, W. Glenn McClung and J. L. Brash, *Acta Biomater.*, 2009, **5**, 1864-1871.
- 39 D. G. Kim, H. Kang, S. Han, H. J. Kim and J. C. Lee, *RSC Adv.*, 2013, **3**, 18071-18081.
- 40 D. Li, H. Chen, S. S. Wang, Z. Q. Wu and J. L. Brash, *Acta Biomater.*, 2011, **7**, 954-958.
- 41 S. Luan, J. Zhao, H. Yang, H. Shi, J. Jin, X. Li, J. Liu, J. Wang, J. Yin and P. Stagnaro, *Colloids Surf., B*, 2012, **93**, 127-134.
- 42 M. Källrot, U. Edlund and A. C. Albertsson, *Biomacromolecules*, 2007, **8**, 2492-2496.
- 43 T. Xiang, W. W. Yue, R. Wang, S. Liang, S. D. Sun and C. S. Zhao, *Colloids Surf., B*, 2013, **110**, 15-21.
- 44 X. L. Liu, W. F. Tong, Z. Q. Wu and W. W. Jiang, *RSC Adv.*, 2013, **3**, 4716-4722.
- 45 S. Q. Nie, J. M. Xue, Y. Lu, Y. Q. Liu, D. S. Wang, S. D. Sun, F. Ran and C. S. Zhao, *Colloids Surf., B*, 2012, **100**, 116-125.
- 46 Y. Xu, M. Takai and K. Ishihara, *Biomaterials*, 2009, **30**, 4930-4938.
- 47 Q. Tu, J. C. Wang, R. Liu, J. He, Y. Zhang, S. Shen, J. Xu, J. Liu, M. S. Yuan and J. Wang, *Colloids Surf., B*, 2013, **102**, 361-370.
- 48 C. Zhang, J. Jin, J. Zhao, W. Jiang and J. Yin, *Colloids Surf., B*, 2013, **102**, 45-52.
- 49 L. Xu, K. Crawford and C. B. Gorman, *Macromolecules*, 2011, **44**, 4777-4782.
- 50 M. D. Wilson and G. M. Whitesides, *J. Am. Chem. Soc.*, 1988, **110**, 8719-8720.
- 51 Z. G. Wang, L. S. Wan and Z. K. Xu, *J. Membr. Sci.*, 2007, **304**, 8-23.
- 52 G. B. Sigal, M. Mrksich and G. M. Whitesides, *J. Am. Chem. Soc.*, 1998, **120**, 3464-3473.
- 53 J. Ma, S. Luan, L. Song, J. Jin, S. Yuan, S. Yan, H. Yang, H. Shi and J. Yin, *ACS Appl. Mater. Interfaces*, 2014, **6**, 1971-1978.
- 54 S. H. Chen, Y. Chang, K. R. Lee, T. C. Wei, A. Higuchi, F. M. Ho, C. C. Tsou, H. T. Ho and J. Y. Lai, *Langmuir*, 2012, **28**, 17733-17742.
- 55 C. Y. Li, W. Yuan, H. Jiang, J. S. Li, F. J. Xu, W. T. Yang and J. Ma, *Bioconjugate Chem.*, 2011, **22**, 1842-1851.